UNIVERSITY OF TORONTO

Institute for Aerospace Studies

Longitudinal Tracking Control Design for Cessna 182 Model

Prepared by
Constantine Boyang Cheng
ID 1002417333
Userid chengboy

Supervised by
Prof. Hugh Liu

December 18th, 2020

1. Introduction of Project

The report demonstrates an autopilot design based on the Cessna-182 aircraft model. The autopilot aims on performing tasks of climbing the aircraft to a new altitude and make a level turn of 90 degrees. The speed control and the pitch attitude control channels are selected for applying the LQR tracking design.

The autopilot is operated based on the non-linear model that indicates the relationships among aerodynamic forces and moments, which is linearized and separated to a longitudinal model and a lateral model based on the properties of each aerodynamic force and moment. The LQR tracking method is applied to the speed control channel and the pitch attitude control channel in the longitudinal model to design the altitude hold autopilot that aims on holding and modifying the altitude and speed of the aircraft. At the same time, PID controllers are utilized in the lateral model for developing the level turn coordinate autopilot for performing the 90-degree-turn. The autopilot is then simulated on both the linearized and non-linear aerodynamics models to verify the performance. Actuation dynamics, model uncertainties and wind gust disturbances are also considered during the testing and simulating processes of the autopilot.

2. Modelling

2.1 Dynamic and Kinematics Equations

For the body-fixed frame $\mathcal{F}_B$, the forces are $\underline{f_B} = m(\underline{\dot{v}_B} + \underline{\omega_B^\times}\underline{v_B})$. Considering the gravity, the following equations expressing the derivatives of linear velocities, $\dot{u}$, $\dot{v}$ and $\dot{w}$, are obtained in $\mathcal{F}_B$:

$$\dot{u} = X/m - qw + rv - g\sin\theta$$
$$\dot{v} = Y/m - ru + pw + g\sin\phi\cos\theta$$
$$\dot{w} = Z/m - pv + qu + g\cos\phi\cos\theta$$

Also, for the body frame $\mathcal{F}_B$, the moments are $\underline{\tau_B} = \underline{\omega_B^\times}\underline{I_B}\underline{\omega_B} + \underline{I_B}\underline{\dot{\omega}_B}$. Since the aircraft is symmetric across the y-axis, the dynamic equations for the derivatives of angular velocities, $\dot{p}$, $\dot{q}$ and $\dot{r}$, are:

$$\dot{p} = \Big(I_{zz}L + I_{xz}N + q\left(p\big(I_{xx} - I_{yy} + I_{zz}\big)I_{xz} + r\big(I_{yy}I_{zz} - I_{zz}^2 - I_{xz}I_{zx}\big)\right)\Big)/(I_{xx}I_{zz} - I_{xz}I_{zx})$$

$$\dot{q} = (M - I_{zx}(p^2 - r^2) - (I_{xx} - I_{zz})pr)/I_{yy}$$

$$\dot{r} = \Big(I_{xx}N + I_{zx}L + q\big(p\big(I_{xx}^2 - I_{xx}I_{yy} + I_{xz}I_{zx}\big) + r\big(I_{yy} - I_{xx} - I_{zz}\big)I_{zx}\big)\Big)/(I_{xx}I_{zz} - I_{xz}I_{zx})$$

For obtaining the equations of the derivatives of displacements, using the rotation matrix from $\mathcal{F}_B$ to $\mathcal{F}_E$, the derivatives of linear motions, $\dot{x}_E$, $\dot{y}_E$ and $\dot{z}_E$, can be expressed as the following linear equations:

$$\begin{bmatrix}\dot{x}_E\\ \dot{y}_E\\ \dot{z}_E\end{bmatrix} = C_{EB}\underline{v_B} = \begin{bmatrix}\cos\theta\cos\psi & \cos\psi\sin\theta\sin\phi - \sin\psi\cos\phi & \cos\psi\sin\theta\cos\phi + \sin\psi\sin\phi\\ \cos\theta\sin\psi & \sin\psi\sin\theta\sin\phi + \cos\psi\cos\phi & \sin\psi\sin\theta\cos\phi - \cos\psi\sin\phi\\ -\sin\theta & \cos\theta\sin\phi & \cos\theta\cos\phi\end{bmatrix}\begin{bmatrix}u\\ v\\ w\end{bmatrix}$$

At the same time, the derivatives of angles, $\dot{\phi}$, $\dot{\theta}$ and $\dot{\psi}$, can be obtained using S_B^{-1}:

$$\begin{bmatrix}\dot{\phi}\\ \dot{\theta}\\ \dot{\psi}\end{bmatrix} = S_B^{-1}\begin{bmatrix}p\\ q\\ r\end{bmatrix} = \begin{bmatrix}1 & \sin\phi\tan\theta & \cos\phi\tan\theta\\ 0 & \cos\phi & -\sin\phi\\ 0 & \sin\phi\sec\theta & \cos\phi\sec\theta\end{bmatrix}\begin{bmatrix}p\\ q\\ r\end{bmatrix}$$

2.2 Approximation of Aerodynamic Forces and Moments

The aerodynamic forces and moments are estimated using aerodynamic derivatives. For the longitudinal forces and moments, ΔX, ΔZ and ΔM, the terms with $v, p, r, \dot{v}, \dot{p}, \dot{r}$ are negligible and δ_e, δ_p, the elevator and throttle inputs, are taken as the control inputs. Also, since $U_e > 0$, $\Delta u = u - U_e$. For the lateral forces and moments, ΔY, ΔL and ΔN, the terms with $u, w, q, \dot{u}, \dot{w}, \dot{q}$ are negligible and δ_a, δ_r, the aileron and rudder inputs, are considered the control inputs. At the same time, the equilibrium states are defined as the following:

$$X_e - W\sin\theta_e = X_e - mg\sin\theta_e = 0 \rightarrow X_e = mg\sin\theta_e$$
$$Z_e + W\cos\theta_e = Z_e + mg\cos\theta_e = 0 \rightarrow Z_e = -mg\cos\theta_e$$
$$M_e = 0, Y_e = 0, L_e = 0, N_e = 0$$

Applying the small perturbation scheme, the aerodynamic forces and moments can be expressed as:

$$\begin{bmatrix} X \\ Z \\ M \end{bmatrix} = \begin{bmatrix} X_e \\ Z_e \\ M_e \end{bmatrix} + \begin{bmatrix} \Delta X \\ \Delta Z \\ \Delta M \end{bmatrix} = \begin{bmatrix} mg\sin\theta_e \\ -mg\cos\theta_e \\ 0 \end{bmatrix} + \begin{bmatrix} X_u & X_w & X_q & X_{\dot{u}} & X_{\dot{w}} & X_{\dot{q}} \\ Z_u & Z_w & Z_q & Z_{\dot{u}} & Z_{\dot{w}} & Z_{\dot{q}} \\ M_u & M_w & M_q & M_{\dot{u}} & M_{\dot{w}} & M_{\dot{q}} \end{bmatrix} \begin{bmatrix} u - U_e \\ w \\ q \\ \dot{u} \\ \dot{w} \\ \dot{q} \end{bmatrix} + \begin{bmatrix} X_{\delta_e} & X_{\delta_p} \\ Z_{\delta_e} & Z_{\delta_p} \\ M_{\delta_e} & M_{\delta_p} \end{bmatrix} \begin{bmatrix} \delta_e \\ \delta_p \end{bmatrix}$$

$$\begin{bmatrix} Y \\ L \\ N \end{bmatrix} = \begin{bmatrix} Y_e \\ L_e \\ N_e \end{bmatrix} + \begin{bmatrix} \Delta Y \\ \Delta L \\ \Delta N \end{bmatrix} = \begin{bmatrix} Y_v & Y_p & Y_r & Y_{\dot{v}} & Y_{\dot{p}} & Y_{\dot{r}} \\ L_v & L_p & L_r & L_{\dot{v}} & L_{\dot{p}} & L_{\dot{r}} \\ N_v & N_p & N_r & N_{\dot{v}} & N_{\dot{p}} & N_{\dot{r}} \end{bmatrix} \begin{bmatrix} v \\ p \\ r \\ \dot{v} \\ \dot{p} \\ \dot{r} \end{bmatrix} + \begin{bmatrix} Y_{\delta_a} & Y_{\delta_r} \\ L_{\delta_a} & L_{\delta_r} \\ N_{\delta_a} & N_{\delta_r} \end{bmatrix} \begin{bmatrix} \delta_a \\ \delta_r \end{bmatrix}$$

The terms where the corresponding aerodynamics derivatives equal to 0 are then neglected from the aerodynamic equations when the configurations of the Cessna-182 model are applied. For example, since $Z_{\dot{q}} = 0$ for the Cessna-182 model, $Z_{\dot{q}}\dot{q}$ term can be neglected from the equations. Also, $\phi \approx 0$ for the longitudinal system. Then, $\dot{w}$ can be determined using the equations of Z to deal with the interactions among the aerodynamic forces and moments and the motions, which is then applied to compute the aerodynamic forces and moments that requires the value of $\dot{w}$ in the s-function:

$$\begin{cases} Z = -mg\cos\theta_e + Z_u(u - U_e) + Z_w w + Z_q q + Z_{\dot{w}}\dot{w} + Z_{\delta_e}\delta_e \\ Z = m(\dot{w} + pv - qu - g\cos\theta) \end{cases}$$

$$\dot{w} = \frac{1}{(m - Z_{\dot{w}})}\left(m(qu - pv) + mg(\cos\theta - \cos\theta_e) + Z_u(u - U_e) + Z_w w + Z_q q + Z_{\delta_e}\delta_e\right)$$

2.3 Linearized Longitudinal and Lateral Equations

Firstly, the following linearized equations can be obtained from the equations in the sections above: [1]

$$X_e + \Delta X - mg(\sin\theta_e + \Delta\theta\cos\theta_e) = m\dot{u}$$
$$Y_e + \Delta Y + mg\Delta\phi\cos\theta_e = m(\dot{v} + U_e r)$$
$$Z_e + \Delta Z + mg(\cos\theta_e - \Delta\theta\sin\theta_e) = m(\dot{w} - U_e q)$$
$$L_e + \Delta L = I_{xx}\dot{p} - I_{zx}\dot{r}, \qquad M_e + \Delta M = I_{yy}\dot{q}, \qquad N_e + \Delta N = -I_{zx}\dot{p} + I_{zz}\dot{r}$$
$$\Delta\dot{\theta} = q, \qquad \Delta\dot{\phi} = p + r\tan\theta_e, \qquad \Delta\dot{\psi} = r\sec\theta_e$$

Then, the state-space formations for the linearized longitudinal and lateral models can be defined as:

$$\begin{bmatrix}\dot{u}\\ \dot{w}\\ \dot{q}\\ \dot{\theta}\end{bmatrix}=\begin{bmatrix} X_u/m & X_w/m & X_q/m & -g\cos\theta_e \\ \dfrac{Z_u}{m-Z_{\dot{w}}} & \dfrac{Z_w}{m-Z_{\dot{w}}} & \dfrac{Z_q+mU_e}{m-Z_{\dot{w}}} & -\dfrac{mg\sin\theta_e}{m-Z_{\dot{w}}} \\ \dfrac{1}{I_{yy}}\left(M_u+\dfrac{Z_u}{m-Z_{\dot{w}}}M_{\dot{w}}\right) & \dfrac{1}{I_{yy}}\left(M_w+\dfrac{Z_w}{m-Z_{\dot{w}}}M_{\dot{w}}\right) & \dfrac{1}{I_{yy}}\left(M_q+\dfrac{Z_q+mU_e}{m-Z_{\dot{w}}}M_{\dot{w}}\right) & -\dfrac{1}{I_{yy}}\left(\dfrac{mg\sin\theta_e}{m-Z_{\dot{w}}}M_{\dot{w}}\right) \\ 0 & 0 & 1 & 0 \end{bmatrix}\begin{bmatrix}u-U_e\\ w\\ q\\ \theta\end{bmatrix}$$

$$+\begin{bmatrix} X_{\delta_e}/m & X_{\delta_p}/m \\ \dfrac{Z_{\delta_e}}{m-Z_{\dot{w}}} & \dfrac{Z_{\delta_p}}{m-Z_{\dot{w}}} \\ \dfrac{1}{I_{yy}}\left(M_{\delta_e}+\dfrac{Z_{\delta_e}}{m-Z_{\dot{w}}}M_{\dot{w}}\right) & \dfrac{1}{I_{yy}}\left(M_{\delta_p}+\dfrac{Z_{\delta_p}}{m-Z_{\dot{w}}}M_{\dot{w}}\right) \\ 0 & 0 \end{bmatrix}\begin{bmatrix}\delta_e\\ \delta_p\end{bmatrix}$$

$$\begin{bmatrix}\dot{v}\\ \dot{p}\\ \dot{r}\\ \dot{\phi}\end{bmatrix}=\begin{bmatrix} Y_v/m & Y_p/m & Y_r/m-U_e & g\cos\theta_e \\ I'_{xx}L_v+I'_{zx}N_v & I'_{xx}L_p+I'_{zx}N_p & I'_{xx}L_r+I'_{zx}N_r & 0 \\ I'_{zz}N_v+I'_{zx}L_v & I'_{zz}N_p+I'_{zx}L_p & I'_{zz}N_r+I'_{zx}L_r & 0 \\ 0 & 1 & \tan\theta_e & 0 \end{bmatrix}\begin{bmatrix}v\\ p\\ r\\ \phi\end{bmatrix}+\begin{bmatrix} Y_{\delta_a}/m & Y_{\delta_r}/m \\ I'_{xx}L_{\delta_a}+I'_{zx}N_{\delta_a} & I'_{xx}L_{\delta_r}+I'_{zx}N_{\delta_r} \\ I'_{zz}N_{\delta_a}+I'_{zx}L_{\delta_a} & I'_{zz}N_{\delta_r}+I'_{zx}L_{\delta_r} \\ 0 & 0 \end{bmatrix}\begin{bmatrix}\delta_a\\ \delta_r\end{bmatrix}$$

Where:

$$I'_{xx}=\frac{I_{zz}}{I_{xx}I_{zz}-I_{zx}^2}, I'_{zz}=\frac{I_{xx}}{I_{xx}I_{zz}-I_{zx}^2}, I'_{zx}=\frac{I_{zx}}{I_{xx}I_{zz}-I_{zx}^2}$$

In this case, since $U_e>0$, $\Delta u=u-U_e$, then it is impossible to approximate Δu as u and the speed state is defined as the difference between the actual speed u and the steady-state speed U_e.

Apply the parameters of Cessna-182 Model to the state-space equations of the linearized longitudinal and lateral models, the following equations are obtained:

$$\begin{bmatrix}\dot{u}\\ \dot{w}\\ \dot{q}\\ \dot{\theta}\end{bmatrix}=\begin{bmatrix}-0.0453 & -0.0571 & 0 & -9.8100\\ -0.2902 & -2.0628 & 65.0354 & 0\\ 0.0112 & -0.2103 & -6.8935 & 0\\ 0 & 0 & 1 & 0\end{bmatrix}\begin{bmatrix}u-U_e\\ w\\ q\\ \theta\end{bmatrix}+\begin{bmatrix}0 & 1.7658\\ -13.4762 & 0\\ -34.9936 & 0\\ 0 & 0\end{bmatrix}\begin{bmatrix}\delta_e\\ \delta_p\end{bmatrix}$$

$$\begin{bmatrix}\dot{v}\\ \dot{p}\\ \dot{r}\\ \dot{\phi}\end{bmatrix}=\begin{bmatrix}-0.1855 & -0.1947 & -66.4445 & 9.8100\\ -0.4540 & -13.0935 & 2.1588 & 0\\ 0.1391 & -0.3624 & -1.2216 & 0\\ 0 & 1 & 0 & 0\end{bmatrix}\begin{bmatrix}v\\ p\\ r\\ \phi\end{bmatrix}+\begin{bmatrix}0 & 5.9132\\ -75.4673 & 4.8444\\ -3.4305 & -10.2440\\ 0 & 0\end{bmatrix}\begin{bmatrix}\delta_a\\ \delta_r\end{bmatrix}$$

From the linearized equations, the eigenvalues are obtained and associated with each dynamic mode:
Longitudinal Short-Period Mode: $-4.4822\pm2.7986i$; Phugoid Mode: $-0.0185\pm0.1708i$
Lateral Spiral Mode: -0.0179; Rolling Mode: -13.1313; Dutch-Roll Mode: $-0.6757\pm3.1826i$

3. Control Design and Implementation

3.1 State-Space Model Defining and Design Requirement

In this chapter, the designs of the speed control and the pitch attitude control will be discussed. The speed control and the pitch attitude control are designed to track the forward speed and the pitching angle commands. The state-space model of the linearized longitudinal system will be considered as the original state-space model for the speed and pitch attitude control designing processes, and no dynamic mode approximation is applied on the state-space formation in this design.

Since the design aims at tracking the speed command (u_c) and pitching angle commands (θ_c), which indicates that a tracking problem is expected to be solved, the tracking errors are defined:

$$e_u = u_c - (u - U_e), \qquad e_\theta = \theta_c - \theta$$

Then, the following integral states can be defined to incorporate the tracking errors in the system:

$$\epsilon_u = \int e_u \rightarrow \dot{\epsilon}_u = e_u = u_c - (u - U_e), \qquad \epsilon_\theta = \int e_\theta \rightarrow \dot{\epsilon}_\theta = e_\theta = \theta_c - \theta$$

For this design task, the tracking control design is conducted using the output feedback. However, since the states are expected to be tracked and measured to evaluate the performance of the autopilot, the outputs are defined as $\underline{y} = \underline{x}$, the augmented output matrix, C_{aug}, of the state-space model is then defined as an identity matrix with the same number of columns and rows as the number of states. Correspondingly, the F matrix of the model is defined as a zero matrix. At the same time, since $\underline{e} = \underline{r} - \underline{z}$, u and θ are incorporated in the performance signal $\underline{z}$. Then, the following system is defined:

$$\underline{\dot{x}} = A_{aug}\underline{x} + B_{aug}\underline{u} + G\underline{r}, \qquad \underline{y} = C_{aug}\underline{x} + F\underline{r}, \qquad \underline{z} = H\underline{x}, \qquad \underline{u} = -K\underline{y}$$

Also, the following actuation dynamics are assumed, where u_e and u_p are the inputs to the actuators:

$$\delta_e(s) = \frac{10}{s+10}u_e \rightarrow \dot{\delta}_e = -10\delta_e + 10u_e, \qquad \delta_p(s) = \frac{15}{s+15}u_p \rightarrow \dot{\delta}_p = -15\delta_p + 15u_p$$

After the actuators are integrated, the states in the model include the states of the linearized longitudinal model, $u - U_e$, w, q and θ; the two inputs, δ_e and δ_p; and the integral of the two tracking errors, ϵ_u and ϵ_θ. Then, the following model is obtained:

$$\underline{\dot{x}} = \begin{bmatrix} \dot{u} \\ \dot{w} \\ \dot{q} \\ \dot{\theta} \\ \dot{\delta}_e \\ \dot{\delta}_p \\ \dot{\epsilon}_u \\ \dot{\epsilon}_\theta \end{bmatrix} = \begin{bmatrix} -0.0453 & -0.0571 & 0 & -9.8100 & 0 & 1.7658 & 0 & 0 \\ -0.2902 & -2.0628 & 65.0354 & 0 & -13.4762 & 0 & 0 & 0 \\ 0.0112 & -0.2103 & -6.8935 & 0 & -34.9936 & 0 & 0 & 0 \\ 0 & 0 & 1 & 0 & 0 & 0 & 0 & 0 \\ 0 & 0 & 0 & 0 & -10 & 0 & 0 & 0 \\ 0 & 0 & 0 & 0 & 0 & -15 & 0 & 0 \\ -1 & 0 & 0 & 0 & 0 & 0 & 0 & 0 \\ 0 & 0 & 0 & -1 & 0 & 0 & 0 & 0 \end{bmatrix} \begin{bmatrix} u - U_e \\ w \\ q \\ \theta \\ \delta_e \\ \delta_p \\ \epsilon_u \\ \epsilon_\theta \end{bmatrix} + \begin{bmatrix} 0 & 0 \\ 0 & 0 \\ 0 & 0 \\ 0 & 0 \\ 10 & 0 \\ 0 & 15 \\ 0 & 0 \\ 0 & 0 \end{bmatrix} \begin{bmatrix} u_e \\ u_p \end{bmatrix} + \begin{bmatrix} 0 & 0 \\ 0 & 0 \\ 0 & 0 \\ 0 & 0 \\ 0 & 0 \\ 0 & 0 \\ 1 & 0 \\ 0 & 1 \end{bmatrix} \begin{bmatrix} u_c \\ \theta_c \end{bmatrix}$$

$$\underline{y} = \underline{x} = diag([1,1,1,1,1,1,1,1])\underline{x}, F = \underline{0}$$

$$\underline{z} = \begin{bmatrix} u \\ \theta \end{bmatrix} = \begin{bmatrix} 1 & 0 & 0 & 0 & 0 & 0 & 0 & 0 \\ 0 & 0 & 0 & 1 & 0 & 0 & 0 & 0 \end{bmatrix} \underline{x}$$

Since the model aims on tracking the speed and pitching angle commands, the design requirements are related to the tracking performances of each channel. The overshoot is expected to be less than 10% and the steady-state tracking error is expected to be less than 5% for all channels in this design to guarantee the capability of the aircraft to perform the climbing and turning tasks successfully. For designs that meet typical design specifications on both the overshoot and the steady-state error, the design that leads to a settling time less than 40 seconds is preferred for all speed and angular velocity channels to ensure a high efficiency. These requirements also apply to cases where noises or disturbances are added to the system.

3.2 Implementation and Verification of LQR Design

In the design processes, the best group of Q and R is selected based on the verification results. The verification process is conducted by evaluating the unit-step responses of each channel in the scope of the design while the closed-loop system for verification is $A_c = A - BKC$ and $B_c = G - BKF$. [1]

Firstly, the identity matrices are selected as Q and R. However, the settling time for the pitching angle channel exceeds 40 seconds, which is slightly longer than expected. Since a larger weight on Q indicates higher importance of the corresponding state, increasing the corresponding diagonal term in Q leads to a shorter settling time but a larger overshoot. To reduce the settling time of the pitch attitude control channel and ensure that the overshoot does not exceed the requirement, the weight associated with ϵ_θ in Q increases to 1000. Also, 5 is picked as the weight of ϵ_u in Q to slightly reduce the settling time of the speed for a larger acceleration of the aircraft. Also, since the weights in R matrix refer to the important of corresponding inputs and the elevator and throttle are considered equally important, R matrix remains the identity matrix in the final design. The final designs for Q and R are the following:

$$Q = diag([1, 1, 1, 1, 1, 1, 5, 1000]), \qquad R = diag([1, 1])$$

By solving the Ricatti equation using Q and R, the following control law K is obtained:

$$K = \begin{bmatrix} 0.2969 & -0.4142 & -3.6319 & -35.8250 & 4.3417 & 0.0229 & -0.4034 & 31.1040 \\ 2.1676 & 0.0007 & -0.0535 & -1.7146 & 0.0343 & 0.5842 & -2.1994 & -5.7045 \end{bmatrix}$$

The design is then verified using unit-step commands, and the step responses are plotted below:

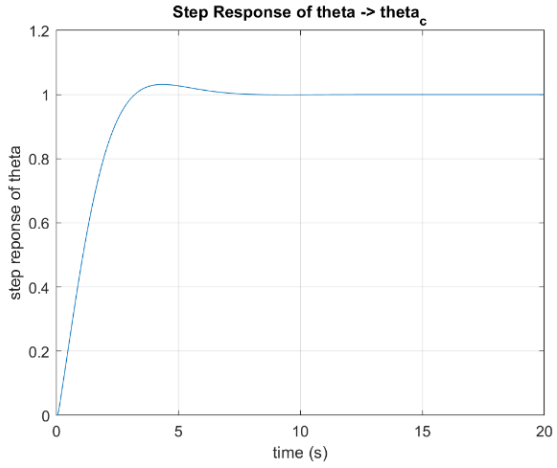

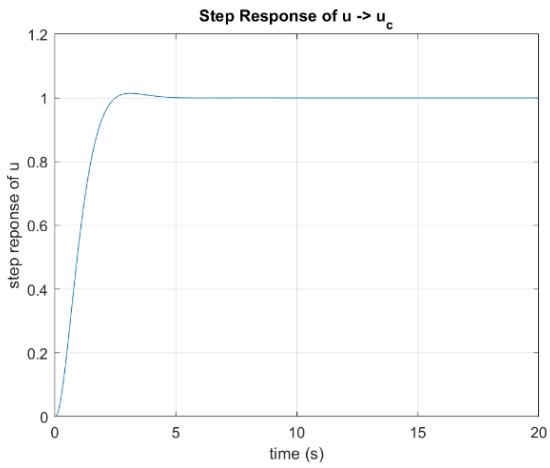

From the plots above, it is obvious that the steady-state errors for both channels are close to 0 and the overshoots for both channels are less than 5%. At the same time, the settling time for both channels is less than 10 seconds, which shows that all design requirements are fulfilled.

3.3 Robustness Analysis

The model uncertainties, noises and disturbances are considered in the robustness analysis. The transfer function of the unmodeled high-frequency dynamics of the first flexible mode, M, is assumed and defined. Also, a wind gust model is assumed as the disturbance to verify the robustness of the closed-loop system.

A multiplicative uncertainty is assumed for the longitudinal model. The unmodeled high-frequency plant dynamics is defined as the following, where $\omega_n = 60$ and $\xi = 0.3$ are selected: [2]

$$M(s) = \frac{\omega_n^2}{s^2 + 2\omega_n\xi s + \omega_n^2} - 1 = \frac{-s^2 - 2\omega_n\xi s}{s^2 + 2\omega_n\xi s + \omega_n^2} = \frac{-s^2 - 36s}{s^2 + 36s + 3600}$$

Also, a wind gust model is created and considered the disturbance. The wind gust model can be defined as the following equation with $L = 3.86\,s$ based on the airspeed and $\sigma = 0.15$ for considering a high-turbulence case: [2][3]

$$\phi_w(\omega) = 2L\sigma^2 \frac{1 + 3L^2\omega^2}{(1 + L^2\omega^2)^2}$$

Then, the singular value of the longitudinal model, $1/M(s)$ and the wind gust $\phi_w(\omega)$ are plotted in the diagram at the right. From the diagram, it is obvious that the lower bound of singular values is greater than 1 (0 dB) at low frequencies and the upper bound of singular values is smaller than 1 at high frequencies, which demonstrates that the model fulfills the desired specifications. Also, $\overline{\sigma}(GK(j\omega)) < \underline{\sigma}(M(j\omega))$ and $\underline{\sigma}(GK(j\omega)) > \phi_w(\omega)$, which indicates that the model presents both high stability robustness and high performance robustness.

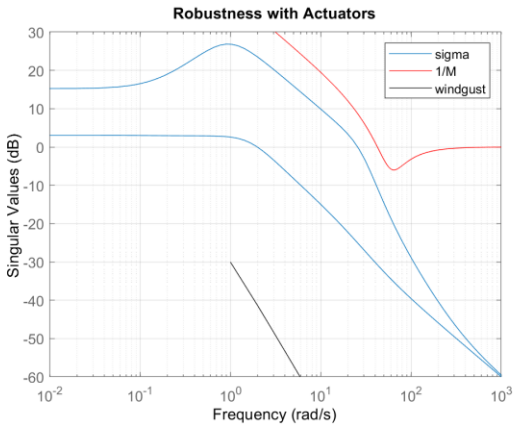

4. Simulation

4.1 Altitude Hold Autopilot Simulation

The altitude hold autopilot is based on the longitudinal model and aims on holding the altitude and speed of the aircraft or modify the altitude and speed of the aircraft. To build an altitude hold autopilot, the altitude, h, is integrated into the states of the longitudinal model. Since the rate of change of the altitude can be expressed by the following equation:

$$\dot{h} = -\Delta z_E = u\sin\theta_e - w\cos\theta_e + U_e\theta\cos\theta_e$$

The longitudinal state-space model with the configurations of Cessna-182 applied can be modified as the following to have the altitude integrated:

$$\begin{bmatrix}\dot{u}\\ \dot{w}\\ \dot{q}\\ \dot{\theta}\\ \dot{h}\end{bmatrix} = \begin{bmatrix}-0.0453 & -0.0571 & 0 & -9.8100 & 0\\ -0.2902 & -2.0628 & 65.0354 & 0 & 0\\ 0.0112 & -0.2103 & -6.8935 & 0 & 0\\ 0 & 0 & 1 & 0 & 0\\ 0 & -1 & 0 & 67 & 0\end{bmatrix}\begin{bmatrix}u - U_e\\ w\\ q\\ \theta\\ h\end{bmatrix} + \begin{bmatrix}0 & 1.7658\\ -13.4762 & 0\\ -34.9936 & 0\\ 0 & 0\\ 0 & 0\end{bmatrix}\begin{bmatrix}\delta_e\\ \delta_p\end{bmatrix}$$

A Simulink model is developed for verifying the performance of the autopilot. Two step-signals are created as the commands of the speed and altitude channels respectively. The final value of the altitude command is set to be 1500 meters, and the final value of the speed command is set to be 67 meters per second, which indicates that the final speed is 67 m/s higher than the equilibrium speed $U_e = 67\,m/s$ and results in $u = 134\,m/s$. The commands are the equilibrium points of the Cessna-182 model.

The gain K_h is applied to convert the altitude command to the pitching angle command. A large value of K_h leads to instability, larger oscillation or drastic rate of change of the pitching angle, and a small value of K_h results in a large steady-state error and a slow climb based on the experimental results. So, $K_h = 0.004$ is picked up. Also, a saturation component is applied to the altitude channel to limit the pitching angle in the range from $-30°$ to $30°$, which is based on the specifications of the Cessna-182 model. [4]

Then, model uncertainties, noises and disturbances are considered in the simulation. The model uncertainty dynamics $M(s)$ is applied to both the speed and altitude channels. Since $\overline{\sigma}(GK(j\omega)) < \underline{\sigma}(M(j\omega))$ is verified in the robustness analysis and $M(s)$ is large at high frequency, $M(s)$ can also be assumed as the filter of the measurement noise. At the same time, the wind gust is applied to the speed and the pitching angle channels as the disturbances. A white noise generator is created, and the wind gust dynamics ϕ_w is used as the weighting function of the disturbance to transfer the white noise to the coloured noise. Since $\sigma = 0.15$ and $L = 3.86$, the transfer function of the wind gust can be defined as:

$$H_w(s) = \sigma\sqrt{\frac{6}{L}}\frac{s + \frac{1}{\sqrt{3}L}}{\left(s^2 + \frac{2s}{L} + \frac{1}{L^2}\right)} = \frac{0.187s + 0.02797}{s^2 + 0.51813s + 0.067116}$$

The simulation results are plotted below:

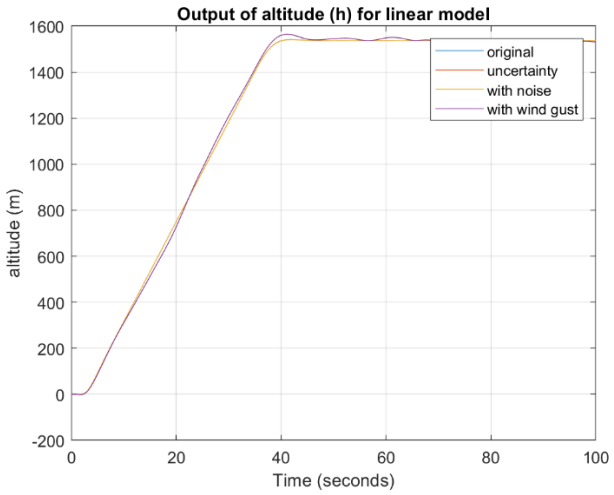

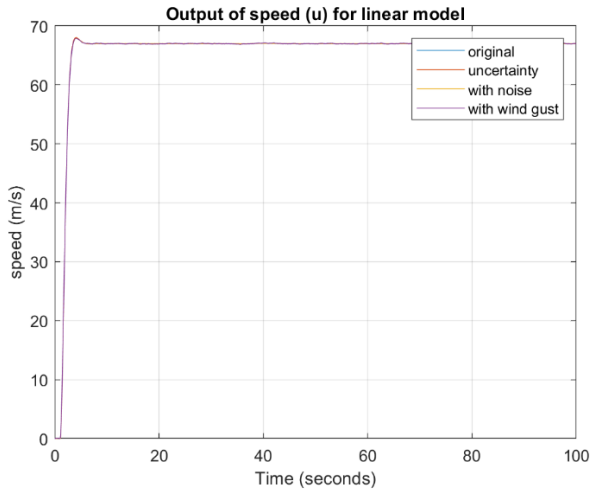

The outputs above show that the steady-state errors for both the altitude and the speed are smaller than 5% and the overshoots for both channels are smaller than 10%. At the same time, the settling time is less than 10 seconds for the speed channel. For the altitude channel, the system settles down in 10 seconds before the steady climb period and reaching the final altitude, which shows that the settling time for the pitching angle is in 10 seconds. Also, the design requirements are still met when the noise or disturbance is applied. Hence, all design requirements are considered fulfilled based on the simulating results.

4.2 Level Turn Coordinate Autopilot Simulation

The level turn coordinate autopilot is based on the lateral model and aims on turning the aircraft steadily at an altitude with a constant speed. In this simulation, the aircraft is controlled to make a 90 degrees level

turn. For the level turn coordinate autopilot, the yawing angle ψ is integrated into the model for verifying the performance of the aircraft on the level turn by tracking the heading. Since the rate of change of the yawing angle is given as the following:

$$\dot{\psi} = r \sec \theta_e$$

Apply the Cessna-182 configurations, the lateral state-space model can be modified as the following to have the yaw angle integrated:

$$\begin{bmatrix} \dot{v} \\ \dot{p} \\ \dot{r} \\ \dot{\phi} \\ \dot{\psi} \end{bmatrix} = \begin{bmatrix} -0.1855 & -0.1947 & -66.4445 & 9.8100 & 0 \\ -0.4540 & -13.0935 & 2.1588 & 0 & 0 \\ 0.1391 & -0.3624 & -1.2216 & 0 & 0 \\ 0 & 1 & 0 & 0 & 0 \\ 0 & 0 & 1 & 0 & 0 \end{bmatrix} \begin{bmatrix} v \\ p \\ r \\ \phi \\ \psi \end{bmatrix} + \begin{bmatrix} 0 & 5.9132 \\ -75.4673 & 4.8444 \\ -3.4305 & -10.2440 \\ 0 & 0 \\ 0 & 0 \end{bmatrix} \begin{bmatrix} \delta_a \\ \delta_r \end{bmatrix}$$

The actuation dynamics for both the roll control and the yaw damper are assumed to be the following:

$$J_a = J_r = 15/(s + 15)$$

Firstly, a PID controller is designed for the yaw damper channel. For the level turn coordinate model, the washout filter for the yaw damper is assumed to be the following:

$$W = s/(s + 1)$$

Then, the root locus of the closed-loop system is plotted to determine the gain. From the root locus of the positive feedback system, the optimal gain selection for the controller is $K_P \approx -0.53$.

Secondly, a PID controller is designed for the roll control channel. $K_\psi = 1$ is picked up to convert the heading command ψ_c to the bank angle command ϕ_c. To both restrict the settling time in 40 seconds and create a relatively smooth turn, $K_P = -0.05$ and $K_D = -0.01$ are picked up. Also, a saturation component is added to the roll channel to limit the bank angle in the range from -0.5 radians to 0.5 radians. [4] At the same time, the wind gust disturbances are then applied to the heading channel to verify the robustness of the autopilot. The wind gust model defined in Chapter 3 is utilized in this case.

The output of the heading channel is shown in the plots at the right. From the results, it is obvious that the steady-state error for the heading channel is nearly 0. At the same time, the overshoot of the heading is smaller than 10%. Also, the optimal settling time for the bank angle after the steady turning period is around 20 seconds (from around T=30s to 50s). When the wind gust disturbance is applied, the overshoot and steady-state error for the heading channel slightly increases, but the requirements are still met. Overall, all requirements are fulfilled by the design.

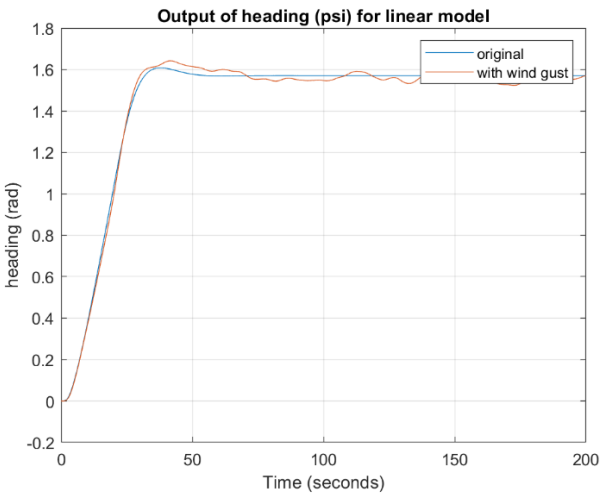

4.3 Non-linear Model Simulation

The dynamic and kinematic equations and the estimated aerodynamic forces and motions are applied to develop the non-linear model. Since $U_e \neq 0$, the speed channel is defined as the speed from the equilibrium, which is $u - U_e$.

To firstly perform an altitude change and then make a 90-degree level turn, the altitude change is conducted at the beginning of the simulation and the step time of commands for both the altitude and the speed channels are set to be T = 1 s. The level turn is then performed after both the altitude and the speed channels are settled down, which is around the 150th second. So, the step time of the heading command ψ_c is set to be T = 150 s. Also, the wind gust disturbances are applied to the speed, the pitching angle and the bank angle channels of the non-linear model. The wind gust model applied in the simulations of linearized models is also utilized in this case.

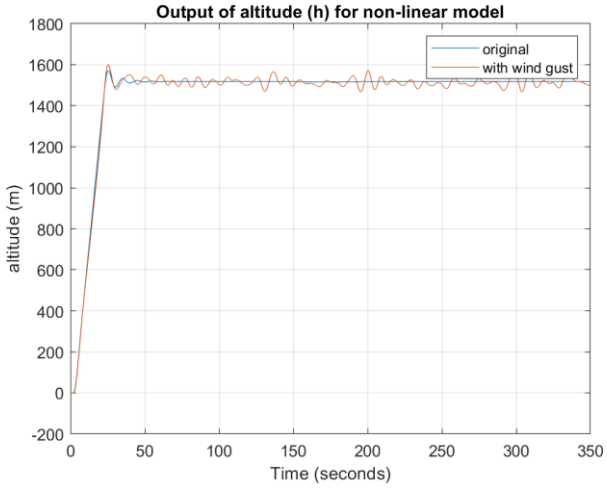

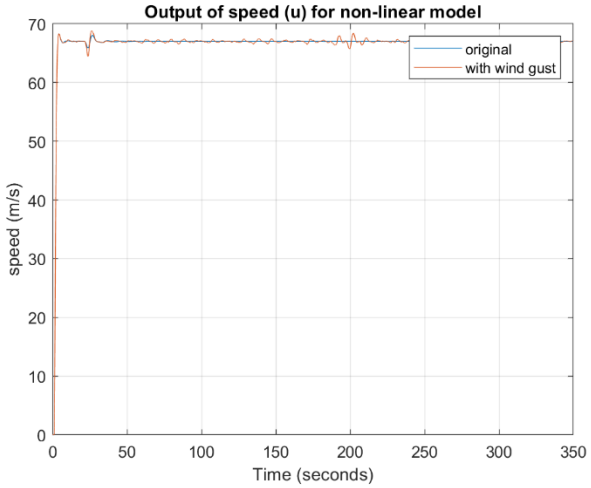

The simulation results for the speed channel and the altitude channel are shown in the plots above. From the results, the steady-state errors for both the altitude and the speed are smaller than 5%, and the overshoots for both channels are smaller than 10%. However, comparing to the simulation results on the linearized model, larger oscillation is presented in both the outputs of the altitude and the speed, which also results in a settling time $T_s \approx 40\ s$ for both the pitching angle and the speed channels. It is obvious that the settling time meets the requirement but is larger than the settling time presented in the simulation results of the linearized models.

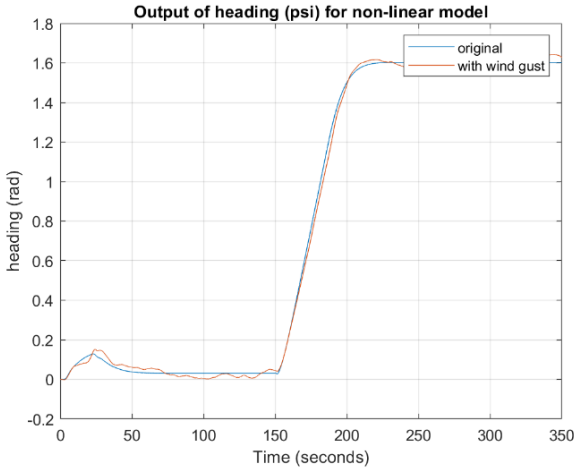

The output for the heading channel is shown in the diagram at the left. From the results, the steady-state error for the heading is smaller than 5%, and there is no overshoot or oscillation presented. Also, the settling time for the bank angle channel is around 20 seconds, which are smaller than the preferred settling time.

From the plots above, the overshoots of steady-state error of each channel increases when the wind gust disturbance is applied. The design requirements are still fulfilled, which shows that the non-linear model is robust enough for handling the specified wind gust disturbance. However, the robustness of the non-linear model is weaker compared to the robustness of the linearized models since the disturbance shows larger impacts on the non-linear model than on the linearized models.

In addition, when using a K_h larger than 0.004 in the altitude channel, the wind gust disturbance results in a divergence of the response and the instability of the model, which is one of the main reasons that the value of K_h is set as 0.004.

5. Conclusion

In the design process, the models are verified by applying step signals as the commands to the pitching angle channel and the speed channel. From the verification results, the overshoots and steady-state errors are close to 0 for both channels and the settling times are smaller than 10 seconds, which shows that all design requirements are met. At the same time, based on the robustness analysis, the singular values of the closed-loop model are large at low frequencies and small at high frequencies. Unmodeled dynamics and wind gust disturbances are also assumed, which give $\overline{\sigma}(GK(j\omega)) < \underline{\sigma}(M(j\omega))$ and $\underline{\sigma}(GK(j\omega)) > \phi_w(\omega)$, and show that the designed model has strong robustness.

In the simulation process, the linearized altitude hold autopilot, level turn coordinate autopilot and the non-linear model are evaluated. Also, the wind gust disturbance defined in the robustness analysis process is applied to all models for verifying the robustness of each model. From the simulating results, all design requirements are fulfilled in each case. The overshoot of the heading channel, which is part of the lateral model, is smaller than the overshoots of the longitudinal channels, but the settling time of the heading channel is larger. Comparing to the linearized models, the simulating results of the non-linear model have larger oscillation and thus larger settling time. Also, the non-linear model is less robust than the linearized models. In conclusion, the results indicate that the design successfully performs the required task, and all design requirements are fulfilled based on the results of the simulations.

6. Reference

[1] H. Liu, Advanced Flight Dynamics Stability and Control, 2020.

[2] B. Stevens, et al., *Aircraft Control and Simulation: Dynamics, Controls Design, and Autonomous Systems*, John Wiley & Sons, Inc., New York, 2016.

[3] F. Russo, et al., "Scaling of Turbulence Intensity for Low-Speed Flow in Smooth Pipes", *Flow Measurement and Instrumentation*, doi: 10.1016/j.flowmeasinst.2016.09.012.

[4] T. Gorski, "Cessna 182 Profiles", Feb. 2018, http://tomgorski.com/asr/Cessna%20182%20Profiles.pdf.

Appendix

Part A: Steps for Deriving Dynamics and Kinematics Equations

For the body-fixed frame $\mathcal{F}_B$, the forces are $\underline{f_B} = m(\underline{\dot{v}_B} + \underline{\omega_B^\times}\underline{v_B})$. Since:

$$\underline{f_B} = \begin{bmatrix} X \\ Y \\ Z \end{bmatrix}, \underline{\dot{v}_B} = \begin{bmatrix} \dot{u} \\ \dot{v} \\ \dot{w} \end{bmatrix}, \underline{\omega_B^\times} = \begin{bmatrix} 0 & -r & q \\ r & 0 & -p \\ -q & p & 0 \end{bmatrix}, \underline{v_B} = \begin{bmatrix} u \\ v \\ w \end{bmatrix}$$

The forces can be expressed as the following linear equations:

$$\begin{bmatrix} X \\ Y \\ Z \end{bmatrix} = m\left(\begin{bmatrix} \dot{u} \\ \dot{v} \\ \dot{w} \end{bmatrix} + \begin{bmatrix} 0 & -r & q \\ r & 0 & -p \\ -q & p & 0 \end{bmatrix}\begin{bmatrix} u \\ v \\ w \end{bmatrix}\right) = m\left(\begin{bmatrix} \dot{u} - rv + qw \\ \dot{v} + ru - pw \\ \dot{w} - qu + pv \end{bmatrix}\right)$$

Considering the gravity, the following equations are obtained in $\mathcal{F}_B$:

$$X = m(\dot{u} + qw - rv + g\sin\theta)$$
$$Y = m(\dot{v} + ru - pw - g\sin\phi\cos\theta)$$
$$Z = m(\dot{w} + pv - qu - g\cos\phi\cos\theta)$$

So, the dynamic equations for $\dot{u}$, $\dot{v}$ and $\dot{w}$ can be expressed as the following:

$$\dot{u} = X/m - qw + rv - g\sin\theta$$
$$\dot{v} = Y/m - ru + pw + g\sin\phi\cos\theta$$
$$\dot{w} = Z/m - pv + qu + g\cos\phi\cos\theta$$

Also, for the body frame $\mathcal{F}_B$, the moments are $\underline{\tau_B} = \underline{\omega_B^\times}\underline{I_B}\underline{\omega_B} + \underline{I_B}\underline{\dot{\omega}_B}$.

Since $\underline{I_B} = \begin{bmatrix} I_{xx} & 0 & -I_{xz} \\ 0 & I_{yy} & 0 \\ -I_{zx} & 0 & I_{zz} \end{bmatrix}$, $\underline{\tau_B} = \begin{bmatrix} L \\ M \\ N \end{bmatrix}$, $\underline{\omega_B} = \begin{bmatrix} p \\ q \\ r \end{bmatrix}$ and $\underline{\omega_B^\times} = \begin{bmatrix} 0 & -r & q \\ r & 0 & -p \\ -q & p & 0 \end{bmatrix}$

The following linear equations are obtained:

$$\begin{bmatrix} L \\ M \\ N \end{bmatrix} = \begin{bmatrix} 0 & -r & q \\ r & 0 & -p \\ -q & p & 0 \end{bmatrix}\begin{bmatrix} I_{xx} & 0 & -I_{xz} \\ 0 & I_{yy} & 0 \\ -I_{zx} & 0 & I_{zz} \end{bmatrix}\begin{bmatrix} p \\ q \\ r \end{bmatrix} + \begin{bmatrix} I_{xx} & 0 & -I_{xz} \\ 0 & I_{yy} & 0 \\ -I_{zx} & 0 & I_{zz} \end{bmatrix}\begin{bmatrix} \dot{p} \\ \dot{q} \\ \dot{r} \end{bmatrix}$$

Then, the following linear equations are obtained:

$$L = I_{xx}\dot{p} - I_{xz}(\dot{r} + pq) - (I_{yy} - I_{zz})qr$$
$$M = I_{yy}\dot{q} - I_{zx}(r^2 - p^2) - (I_{zz} - I_{xx})pr$$
$$N = I_{zz}\dot{r} - I_{zx}(\dot{p} - qr) - (I_{xx} - I_{yy})pq$$

Then, by solving the linear equations, the dynamic equations for $\dot{p}$, $\dot{q}$ and $\dot{r}$ are the following:

$$\dot{p} = \left(I_{zz}L + I_{xz}N + q\left(p(I_{xx} - I_{yy} + I_{zz})I_{xz} + r(I_{yy}I_{zz} - I_{zz}^2 - I_{xz}I_{zx})\right)\right)/(I_{xx}I_{zz} - I_{xz}I_{zx})$$

$$\dot{q} = (M - I_{zx}(p^2 - r^2) - (I_{xx} - I_{zz})pr)/I_{yy}$$

$$\dot{r} = \left(I_{xx}N + I_{zx}L + q(p(I_{xx}^2 - I_{xx}I_{yy} + I_{xz}I_{zx}) + r(I_{yy} - I_{xx} - I_{zz})I_{zx})\right)/(I_{xx}I_{zz} - I_{xz}I_{zx})$$

For obtaining $\dot{x}_E$, $\dot{y}_E$ and $\dot{z}_E$, the following transformation can be applied from $\mathcal{F}_B$ to $\mathcal{F}_E$:

$$\underline{v}_E = \begin{bmatrix} \dot{x}_E \\ \dot{y}_E \\ \dot{z}_E \end{bmatrix} = C_{EB}\underline{v}_B = C_{EB}\begin{bmatrix} u \\ v \\ w \end{bmatrix}$$

The rotation matrix from $\mathcal{F}_B$ to $\mathcal{F}_E$ can be expressed as the following:

$$C_{EB} = \begin{bmatrix} \cos\psi & -\sin\psi & 0 \\ \sin\psi & \cos\psi & 0 \\ 0 & 0 & 1 \end{bmatrix}\begin{bmatrix} \cos\theta & 0 & \sin\theta \\ 0 & 1 & 0 \\ -\sin\theta & 0 & \cos\theta \end{bmatrix}\begin{bmatrix} 1 & 0 & 0 \\ 0 & \cos\phi & -\sin\phi \\ 0 & \sin\phi & \cos\phi \end{bmatrix}$$

$$= \begin{bmatrix} \cos\theta\cos\psi & \cos\psi\sin\theta\sin\phi - \sin\psi\cos\phi & \cos\psi\sin\theta\cos\phi + \sin\psi\sin\phi \\ \cos\theta\sin\psi & \sin\psi\sin\theta\sin\phi + \cos\psi\cos\phi & \sin\psi\sin\theta\cos\phi - \cos\psi\sin\phi \\ -\sin\theta & \cos\theta\sin\phi & \cos\theta\cos\phi \end{bmatrix}$$

Then, $\dot{x}_E$, $\dot{y}_E$ and $\dot{z}_E$ can be expressed by the following linear equations:

$$\begin{bmatrix} \dot{x}_E \\ \dot{y}_E \\ \dot{z}_E \end{bmatrix} = \begin{bmatrix} \cos\theta\cos\psi & \cos\psi\sin\theta\sin\phi - \sin\psi\cos\phi & \cos\psi\sin\theta\cos\phi + \sin\psi\sin\phi \\ \cos\theta\sin\psi & \sin\psi\sin\theta\sin\phi + \cos\psi\cos\phi & \sin\psi\sin\theta\cos\phi - \cos\psi\sin\phi \\ -\sin\theta & \cos\theta\sin\phi & \cos\theta\cos\phi \end{bmatrix}\begin{bmatrix} u \\ v \\ w \end{bmatrix}$$

For $\dot{\phi}$, $\dot{\theta}$ and $\dot{\psi}$, the following relationship holds:

$$\begin{bmatrix} p \\ q \\ r \end{bmatrix} = \begin{bmatrix} 1 & 0 & -\sin\theta \\ 0 & \cos\phi & \sin\phi\cos\theta \\ 0 & -\sin\phi & \cos\phi\cos\theta \end{bmatrix}\begin{bmatrix} \dot{\phi} \\ \dot{\theta} \\ \dot{\psi} \end{bmatrix} \triangleq S_B \begin{bmatrix} \dot{\phi} \\ \dot{\theta} \\ \dot{\psi} \end{bmatrix}$$

The inverse of S_B matrix can be computed as:

$$S_B^{-1} = \begin{bmatrix} 1 & \sin\phi\sin\theta/\cos\theta & \cos\phi\sin\theta/\cos\theta \\ 0 & \cos\phi & -\sin\phi \\ 0 & \sin\phi/\cos\theta & \cos\phi/\cos\theta \end{bmatrix} = \begin{bmatrix} 1 & \sin\phi\tan\theta & \cos\phi\tan\theta \\ 0 & \cos\phi & -\sin\phi \\ 0 & \sin\phi\sec\theta & \cos\phi\sec\theta \end{bmatrix}$$

Then, $\dot{\phi}$, $\dot{\theta}$ and $\dot{\psi}$ can be obtained using the following linear equations:

$$\begin{bmatrix} \dot{\phi} \\ \dot{\theta} \\ \dot{\psi} \end{bmatrix} = S_B^{-1}\begin{bmatrix} p \\ q \\ r \end{bmatrix} = \begin{bmatrix} 1 & \sin\phi\tan\theta & \cos\phi\tan\theta \\ 0 & \cos\phi & -\sin\phi \\ 0 & \sin\phi\sec\theta & \cos\phi\sec\theta \end{bmatrix}\begin{bmatrix} p \\ q \\ r \end{bmatrix}$$

Part B: Steps for Model Linearization

Assuming small perturbation, the following equations and equilibrium states are obtained:

$$\sin(\theta_e + \Delta\theta) \approx \sin\theta_e + \Delta\theta\cos\theta_e$$

$$\cos(\theta_e + \Delta\theta) \approx \cos\theta_e - \Delta\theta\sin\theta_e$$

$$u_e = U_e, v_e = 0, w_e = 0, p_e = 0, q_e = 0, r_e = 0, \theta_e = \theta_e, \phi_e = 0$$

For longitudinal equations, assuming $\phi = 0$ and $v, p, r, \dot{v}, \dot{p}, \dot{r}$ are negligible, and for lateral equations, $u, w, q, \dot{u}, \dot{w}, \dot{q}$ are negligible. Then, the linearized equations for the aerodynamic forces and moments are:

$$X = X_e + \Delta X = m(\dot{u} + qw - rv + g\sin\theta) = m\big(\dot{u} + g(\sin\theta_e + \Delta\theta\cos\theta_e)\big)$$

$$Y = Y_e + \Delta Y = m(\dot{v} + ru - pw - g\sin\phi\cos\theta) = m(\dot{v} + rU_e - g\Delta\phi\cos\theta_e)$$

$$Z = Z_e + \Delta Z = m(\dot{w} + pv - qu - g\cos\phi\cos\theta) = m\big(\dot{w} - qU_e - g(\cos\theta_e - \Delta\theta\sin\theta_e)\big)$$
$$L = L_e + \Delta L = I_{xx}\dot{p} - I_{xz}(\dot{r} + pq) - \big(I_{yy} - I_{zz}\big)qr = I_{xx}\dot{p} - I_{xz}\dot{r}$$
$$M = M_e + \Delta M = I_{yy}\dot{q} - I_{zx}(r^2 - p^2) - (I_{zz} - I_{xx})pr = I_{yy}\dot{q}$$
$$N = N_e + \Delta N = I_{zz}\dot{r} - I_{zx}(\dot{p} - qr) - \big(I_{xx} - I_{yy}\big)pq = I_{zz}\dot{r} - I_{zx}\dot{p}$$

Rearrange the equations, the following equations are obtained:

$$X_e + \Delta X - mg(\sin\theta_e + \Delta\theta\cos\theta_e) = m\dot{u}$$
$$Y_e + \Delta Y + mg\Delta\phi\cos\theta_e = m(\dot{v} + U_e r)$$
$$Z_e + \Delta Z + mg(\cos\theta_e - \Delta\theta\sin\theta_e) = m(\dot{w} - U_e q)$$
$$L_e + \Delta L = I_{xx}\dot{p} - I_{zx}\dot{r}, \qquad M_e + \Delta M = I_{yy}\dot{q}, \qquad N_e + \Delta N = -I_{zx}\dot{p} + I_{zz}\dot{r}$$
$$\Delta\dot{\theta} = q, \qquad \Delta\dot{\phi} = p + r\tan\theta_e\,, \qquad \Delta\dot{\psi} = r\sec\theta_e$$

So, the longitudinal equation can be expressed as:

$$\begin{bmatrix} -X_u & -X_w & -X_q & mg\cos\theta_e \\ -Z_u & -Z_w & -(mU_e + Z_q) & mg\sin\theta_e \\ -M_u & -M_w & -M_q & 0 \\ 0 & 0 & -1 & 0 \end{bmatrix}\begin{bmatrix} u - U_e \\ w \\ q \\ \theta \end{bmatrix} + \begin{bmatrix} (m - X_{\dot{u}}) & -X_{\dot{w}} & -X_{\dot{q}} & 0 \\ -Z_{\dot{u}} & (m - Z_{\dot{w}}) & -Z_{\dot{q}} & 0 \\ -M_{\dot{u}} & -M_{\dot{w}} & (I_{yy} - M_{\dot{q}}) & 0 \\ 0 & 0 & 0 & 1 \end{bmatrix}\begin{bmatrix} \dot{u} \\ \dot{w} \\ \dot{q} \\ \dot{\theta} \end{bmatrix} = \begin{bmatrix} X_{\delta_e} & X_{\delta_p} \\ Z_{\delta_e} & Z_{\delta_p} \\ M_{\delta_e} & M_{\delta_p} \\ 0 & 0 \end{bmatrix}\begin{bmatrix} \delta_e \\ \delta_p \end{bmatrix}$$

The lateral equation can be expressed as:

$$\begin{bmatrix} -Y_v & -Y_p & mU_e - Y_r & -mg\cos\theta_e \\ -L_v & -L_p & -L_r & 0 \\ -N_v & -N_p & -N_r & 0 \\ 0 & -1 & -\tan\theta_e & 0 \end{bmatrix}\begin{bmatrix} v \\ p \\ r \\ \phi \end{bmatrix} + \begin{bmatrix} (m - Y_{\dot{v}}) & -Y_{\dot{p}} & -Y_{\dot{r}} & 0 \\ -L_{\dot{v}} & (I_{xx} - L_{\dot{p}}) & -(I_{zx} + L_{\dot{r}}) & 0 \\ -N_{\dot{v}} & -(I_{zx} + N_{\dot{p}}) & (I_{zz} - N_{\dot{r}}) & 0 \\ 0 & 0 & 0 & 1 \end{bmatrix}\begin{bmatrix} \dot{v} \\ \dot{p} \\ \dot{r} \\ \dot{\phi} \end{bmatrix} = \begin{bmatrix} Y_{\delta_a} & Y_{\delta_r} \\ L_{\delta_a} & L_{\delta_r} \\ N_{\delta_a} & N_{\delta_r} \\ 0 & 0 \end{bmatrix}\begin{bmatrix} \delta_a \\ \delta_r \end{bmatrix}$$

Part C: Verification Results with Identity Q and R

The step responses for the speed and pitching angle channels when identity matrices are set to be Q and R are shown in the following diagrams:

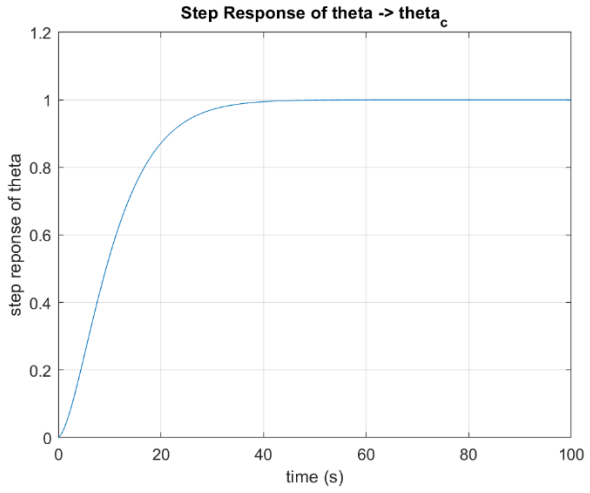

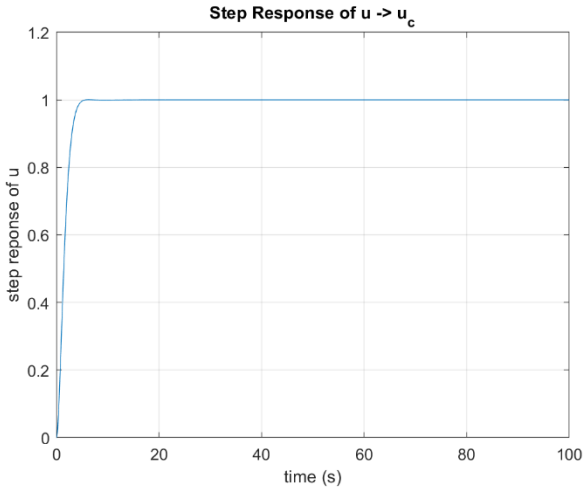

From the plots above, it is obvious that the overshoots and steady-state errors are close to 0. However, the settling time for the pitching angle channel exceeds 40 seconds, which is slightly longer than expected.

Part D: Selection of Noises and Disturbance

A multiplicative uncertainty is assumed for the longitudinal model. The transfer function of the unmodeled high-frequency plant dynamics is defined as the following, where $\omega_n = 60,\ \xi = 0.3$ are selected:

$$M(s) = \frac{\omega_n^2}{s^2 + 2\omega_n\xi s + \omega_n^2} - 1 = \frac{-s^2 - 2\omega_n\xi s}{s^2 + 2\omega_n\xi s + \omega_n^2} = \frac{-s^2 - 36s}{s^2 + 36s + 3600}$$

Then, the unmodeled dynamics are applied to the plant as the following: (Citation)

$$G'(s) = \big(1 + M(s)\big)G(s)$$

Where $G(s)$ denotes the rigid dynamics. Then $\big(1 + M(s)\big)$ can be represented as the following:

$$1 + M(s) = \frac{\omega_n^2}{s^2 + 2\omega_n\xi s + \omega_n^2} = \frac{3600}{s^2 + 36s + 3600}$$

Also, the wind gust is considered the disturbance of the model. According to *Mil. Spec. 1797* (1987), the wind gust can be represented by the following equation:

$$\phi_w(\omega) = 2L\sigma^2 \frac{1 + 3L^2\omega^2}{(1 + L^2\omega^2)^2}$$

Since in the high-turbulence cases, the turbulence intensity σ are normally from 5% to 20%, then $\sigma = 0.15$ is picked. For the turbulence scale length divide by the true airspeed L, a turbulence scale length of 1700 ft is assumed. Since the airspeed is $u = \Delta u + U_e = 67 + 67 = 134\ m/s \approx 440\ fps$, $L = 1700/440 = 3.86\ s$ is assumed.

To get the transfer function of the wind gust, the frequency domain equation of the wind gust can be converted to the following:

$$\phi_w(s) = 2L\sigma^2 \frac{\big(1 + \sqrt{3}Ls\big)\big(1 - \sqrt{3}Ls\big)}{(1 + Ls)^2(1 - Ls)^2} = H_w(s)H_w(-s)$$

$$H_w(s) = \sqrt{2L}\,\sigma \frac{\big(1 + \sqrt{3}Ls\big)}{(1 + Ls)^2} = \sigma\sqrt{\frac{6}{L}}\frac{\left(\frac{1}{\sqrt{3}L} + s\right)}{\left(s + \frac{1}{L}\right)^2} = \sigma\sqrt{\frac{6}{L}}\frac{s + \frac{1}{\sqrt{3}L}}{\left(s^2 + \frac{2s}{L} + \frac{1}{L^2}\right)}$$

Since $\sigma = 0.15$ and $L = 3.86$ are picked, the transfer function of the wind gust can be represented as:

$$H_w(s) = \sigma\sqrt{\frac{6}{L}}\frac{s + \frac{1}{\sqrt{3}L}}{\left(s^2 + \frac{2s}{L} + \frac{1}{L^2}\right)} = \frac{0.187s + 0.02797}{s^2 + 0.51813s + 0.067116}$$

Part E: PID Design for Level Turn Coordinate Autopilot

Firstly, a PID controller is designed for the yaw damper channel. For the level turn coordinate model, the washout filter for the yaw damper is assumed to be the following:

$$W = s/(s + 1)$$

Then, the root locus of the closed-loop system is plotted to determine the gain. The root locus for the negative feedback and positive feedback systems from the input r to the output r_c are plotted below.

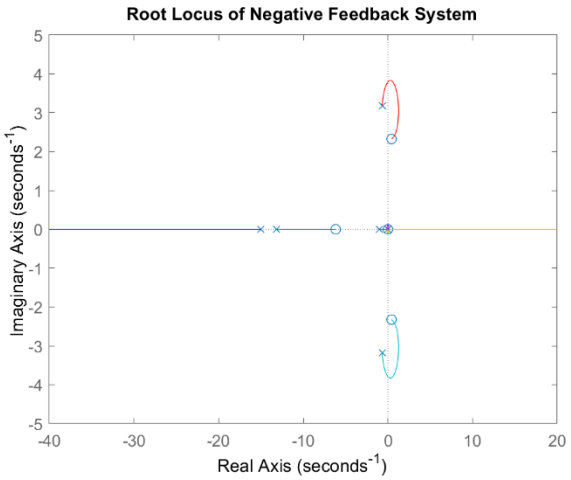

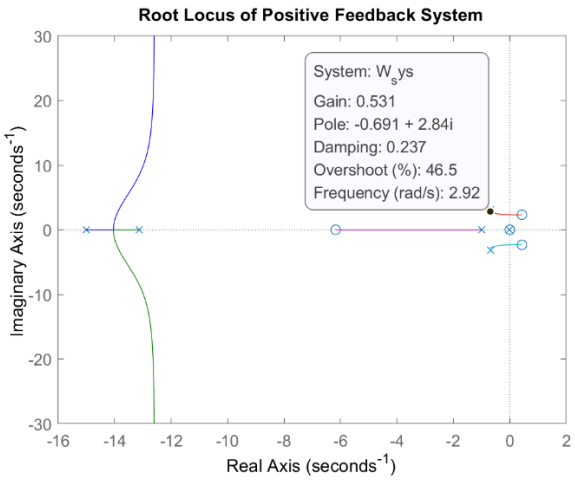

From the plots above, since the root locus of the negative feedback system point towards the positive and negative infinite, the positive feedback system is expected, which means that the gain of the P_D controller is expected to be negative. From the root locus of the positive feedback system, the optimal gain selection for the controller is $K_P \approx -0.53$.

Secondly, a PID controller is designed for the roll control channel. At a coordinate turn, assuming $\theta = 0$, the following equations hold:

$$\begin{cases} mg = L\cos\phi \\ mu\dot{\psi} = L\sin\phi\cos\theta \end{cases}$$

Then, the relation between the roll angle and the rate of change of the yaw angle can be determined:

$$\dot{\psi} = \frac{g}{u}\tan\phi$$

In this simulation, the airspeed $u = \Delta u + U_e = 67 + 67 = 134\ m/s$, then $\dot{\psi} = \frac{g}{u}\tan\phi = \frac{9.8}{134}\tan\phi \rightarrow \phi \approx \frac{134}{9.8}\dot{\psi} = 13.68\dot{\psi}$ since $\phi \ll 1$ for most cases. Then, pick $\tau = 13.68$, $\phi \approx \frac{13.68}{13.68}\psi = \psi$, which means that $K_\psi = 1$.

For the PID controller in the roll channel, K_P and K_D are used as the gains applied to the roll angle ϕ and the rolling rate p. Since the increasing of the absolute values of K_P leads to the increasing of roll angle and the decreasing of the absolute values of K_P results in the increasing of the settling time, $K_P = -0.05$ are picked to restrict the settling time to be less than 40 seconds. Then, the weight $K_D = -0.01$ is assigned to the rolling rate to reduce the rate of change of the bank angle to create a relatively smooth turn. Also, a saturator is added in the roll channel to limit the bank angle in the range from -0.5 radians to 0.5 radians (around 30 degrees), which are the limitations for bank angles for Cessna-182.